energies

MDPI

Article

Experimental Study on Performance of a Containerized 3 MWh High-Temperature Solid Heat Storage and Heat Supply System

Dajiang Guo [1], Hongmei Yin [2,*], Rujie Liu [1], Lin Wang [2], Ziwei Wang [2] and Liming Yang [2]

[1] Three Gorges Electric Energy Co., Ltd., Wuhan 430021, China
[2] Science and Technology Research Institute, China Three Gorges Corporation, Beijing 101199, China
* Correspondence: yin_hongmei@ctg.com.cn; Tel.: +86-13512928976

Abstract

Containerized high-temperature solid heat storage is a promising solution for flexible co-supply of steam and hot water. This paper conducts an experimental study on a 3 MWh containerized high-temperature solid heat storage and supply system, which can simultaneously provide saturated/superheated steam and hot water. High-density magnesia bricks are used as the thermal storage medium and heated to over 800 °C using off-peak electricity or curtailed renewable energy. Circulating air is driven through the saturated and superheated exchange sections successively by variable-frequency fans, realizing on-demand output of thermal energy. The size of the integrated equipment is 11.8 m × 2.13 m × 2.18 m. Experiments were conducted under direct electric heating mode and thermal storage mode. In direct electric heating mode, the storage is kept at 900 °C. As the circulating air flow increases, the inlet/outlet air temperature difference decreases from 600 °C to 300 °C at the saturated section, and from 350 °C to 70 °C at the superheated section, whereas the output power is increased. In thermal storage mode, an adaptive air-volume regulation strategy was used to maintain stable-power release despite the temperature drop of storage bricks. A complete 24 h storage/release cycle test shows that the effective heat storage capacity is 3.14 MWh, the electro-thermal conversion efficiency is 97.84%, and the superheated steam above 450 °C can be stably supplied.

Keywords: high-temperature solid heat storage; combined steam and hot water supply; cogeneration; off-peak electricity utilization; thermal storage efficiency

1. Introduction

As advances are made in global climate governance and carbon neutrality commitments of various countries are implemented, issues including wind and solar curtailment and grid operational challenges are induced by the rapid expansion of installed wind and photovoltaic (PV) capacity owing to the intermittent and fluctuating nature of such renewable power sources. Energy storage is regarded as critical for the accommodation of renewable energy. The intermittent fluctuations of wind and photovoltaic power can be smoothed, curtailment issues can be mitigated, and the grid's ability to absorb new energy power can be improved. At present, energy storage technologies include electrochemical energy storage, electrolytic hydrogen production, compressed air energy storage, gravity energy storage and high-temperature solid heat storage. Thermal demands in industrial and civil sectors are receiving widespread attention globally. Compared with electric energy storage, thermal energy storage technologies can be directly matched with thermal loads, and remarkable advantages

Check for updates

Academic Editor: Qiyao Yu

Received: 6 October 2026
Revised: 25 October 2026
Accepted: 28 October 2026
Published: 30 October 2026

Copyright: © 2026 by the authors. Licensee MDPI, Basel, Switzerland. This article is an open access article distributed under the terms and conditions of the Creative Commons Attribution (CC BY) license.

are demonstrated in promoting renewable heat accommodation and cutting fossil fuel consumption, making thermal energy storage a research hotspot in the energy sector.

High-temperature solid heat storage, in which heat is stored using valley electricity or surplus renewable energy for subsequent release, is characterized by high storage density, long service life, low cost, and environmental friendliness. It is regarded as an effective approach to improve power system flexibility and facilitate the deep integration of renewable power. Great application potential is demonstrated in scenarios including industrial steam supply, regional clean heating, and combined heat and power (CHP) systems for industrial parks. Current research on high-temperature solid heat storage technology focuses on heat storage materials, heat exchange structures, system integration, and operational strategies. Luckywell reviews research work on solid-state sensible heat storage systems focusing on the solid materials being used for heat storage applications [1]. The application progress of thermal energy storage technology in the field of storage heating and heat-power decoupling technology is introduced by Zeng [2]. The research status and progress of solid heat storage materials and device structures are summarized by Ma [3].

A large body of research has focused on the stable production of saturated steam to meet the continuous demand for steam with specific pressure levels in industrial processes. On one hand, researchers are devoted to improving the heat transfer performance of the heat storage body itself, for example, by optimizing the flow channel structure of heat storage bricks or developing novel heat storage materials, so as to enhance the heat exchange intensity between the heat storage body and heat transfer fluid [4–7]. Relevant experiments show that the maximum temperature difference of the solid heat storage unit is about 60 K after 8 h of charging; when heating elements are arranged centrally, the temperature difference is as low as 20 K, with radiation heat transfer accounting for 95%, and increasing the proportion of air ducts can improve temperature uniformity [8]. On the other hand, research has extended to the system operation and regulation level. Through experiments and analysis, the influence laws of operating parameters (including ventilation flow rate and temperature) on steam output characteristics have been clarified, and targeted technical optimization schemes for air supply systems, convection tube bundles, and even the entire solid heat storage electric boiler have been put forward accordingly [9]. The output steam temperature of conventional solid heat storage devices is no higher than 200 °C, and ventilation flow rate and feed water flow need to be dynamically matched in the late heat release stage [10]. The optimization of the air supply system in an electric-heated solid thermal storage unit effectively enhances the uniformity index and flow velocity distribution of the air supply [11].

In the application scenarios of regional clean heating and building heat supply, research priorities focus on the effective coupling of HTSHS systems with hot water heating circuits, so as to improve heating quality, system flexibility, and regulation capability. Relevant research progress is characterized by the integration of multiple technical paths and systematic optimization. Some studies have explored the synergistic operation of heat storage systems with other renewable energy sources (such as solar energy and medium-deep geothermal energy), so as to improve long-term operation performance and energy utilization rate through composite heat storage schemes. Data from a 120 MW PV-supported solid heat storage project in Xinjiang show that the multi-energy synergistic mode can accommodate 354 million kWh of surplus new energy power annually, with an annual carbon emission reduction of 465,000 tons [12,13]. Meanwhile, researchers have attached great importance to the efficiency of heat exchange links. For the gas/water heat exchange process, existing studies have verified, through experiments and numerical simulations, the performance improvement effect of enhanced heat transfer structures (such as gradient tree-shaped fins and snowflake-shaped longitudinal ribs) on latent heat or sensible heat storage units.

Experimental data show that such enhanced heat transfer measures as adding fins and optimizing flow channels can improve gas/water heat exchange efficiency by 10–15%, and the actual heat storage capacity of the heat storage body can reach 96% of the theoretical design value [14,15]. In addition, with the increase in system complexity, the research perspective has expanded from single equipment optimization to system scheduling and operation optimization, taking distribution network power constraints and heating reliability into account, and proposing electro-thermal coordinated optimal scheduling methods to meet multi-objective demands. Simulation results show that the electro-thermal coordinated optimal scheduling considering grid constraints can increase the new energy accommodation rate by more than 15%, reduce the comprehensive energy cost by about 20%, and achieve a heating reliability rate of 99.9% [16,17].

To achieve higher-grade thermal energy output and expand applications in power generation or high-end industrial fields, scholars have in recent years focused increasingly on superheated steam preparation technologies and overall system integration schemes. Relevant progress is mainly reflected in the realization of cascade energy utilization and energy grade upgrading through system-level design. In terms of technical paths, researchers mainly explore schemes such as the series arrangement of multi-stage heat exchangers, or the introduction of intermediate heat transfer media such as heat transfer oil, aiming to efficiently utilize the heat in different temperature ranges released by the heat storage body. Specific studies cover performance tests of key components such as finned shell-and-tube heat exchangers, as well as optimization analysis of the charging process of heat storage units, aiming to improve the performance of each heat transfer link. MW-level pilot experiments verify that after optimizing the charging process and heat exchanger structure, the temperature range of solid particle heat storage exceeds 650 °C, 48 h of continuous stable operation can be achieved, and the heat storage and release efficiency exceeds 90% [18,19]. More importantly, research is no longer limited to technical feasibility verification, but extends to the comprehensive evaluation of integrated systems, including structural analysis, operation mechanism discussion and techno-economic analysis of superheated steam power generation systems based on molten salt or solid heat storage, so as to evaluate their practical benefits and application potential. Economic calculations show that the unit heat storage cost of the HTSHS superheated steam system is about 200–400 yuan/kWh, the steam supply cost per kWh is 30–40% lower than that of gas-fired boilers, and the static payback period is about 4–6 years [20,21]. These studies indicate that HTSHS technology is developing towards multi-function, high operating parameters and systematic integration.

However, limited by the complexity and control difficulty of heat exchange section, most solutions lack a systematic design which is capable of on-demand outputting of saturated/superheated steam and water. It is particularly noteworthy that most studies are focused on stationary large-scale heat storage installations. Few investigations have been reported on highly integrated, mobile modular platforms for combined saturated steam and hot water supply.

To solve this problem, this study developed a containerized 3 MWh high-temperature solid heat storage and supply system. To meet the requirements for on-demand output of hot water and steam as well as rapid installation, a system with multi-stage heat storage, series heat exchange and adaptive air volume regulation was constructed. The drawbacks of conventional solid heat storage devices, such as single function and large footprint, were overcome. Experiments under two typical operating modes, i.e., direct electric heating steam supply mode and thermal storage mode, were carried out. The influence of circulating air volume on heat exchange efficiency and output power, as well as the role of adaptive air volume adjustment in maintaining stable-power energy supply, was investigated. The

research results can provide technical support for distributed energy supply and grid peak shaving.

2. Materials and Methods

2.1. System Introduction

The 3 MWh high-temperature solid heat storage and supply system mainly consists of a thermal storage tank, steam and water system, and hot air system. The thermal storage tank mainly includes an electric heater, saturated-section solid heat body and superheated-section heat storage body. The steam and water system mainly includes a water tank, water pump, saturated heater, superheater, saturated steam/hot water valve, and superheat steam valve. The system process is shown in Figure 1. The integrated equipment of the 3 MWh high-temperature solid heat storage and supply system is shown in Figure 2. The dimensions of the equipment are 11.8 m in length, 2.13 m in width and 2.18 m in height.

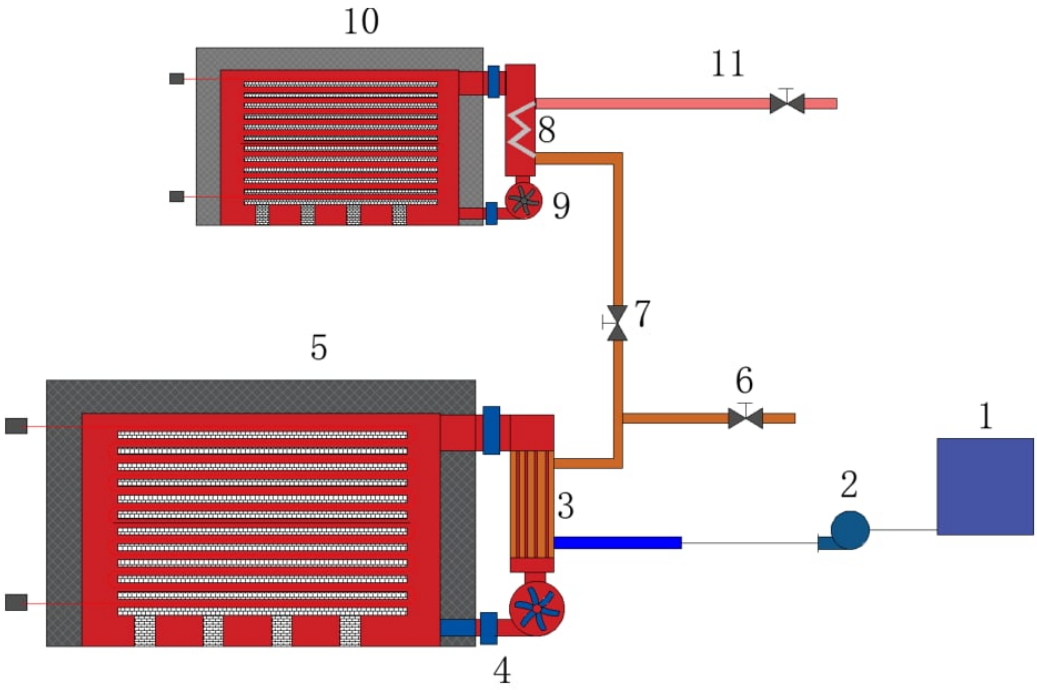


Figure 1. Structure of high-temperature solid heat storage and supply system. 1 Water tank, 2 Water pump, 3 Saturated heater, 4 Hot air fan, 5 Saturated-section solid heat storage unit, 6 Saturated steam/hot water outlet valve, 7 Steam stop valve, 8 Superheater, 9 Hot air fan, 10 Superheated-section high-temperature heat storage unit, 11 Back-pressure valve.

The thermal storage bricks are made of magnesium oxide and stacked to form air flow channels. The magnesia brick has a magnesia content of over 85%, with an apparent density of 2950 kg/m^3, a thermal conductivity of 4.52 W/(m·K), a specific heat capacity of 1.09 kJ/(kg·K), and a volumetric heat capacity of 797 kw·h/m^3. Each high-temperature thermal storage brick has dimensions of 200 mm × 200 mm × 90 mm. Two semi-circular holes with a radius of 25 mm are fabricated on the 200 mm × 90 mm surface for embedding resistance wires. The geometric model of the thermal storage brick is illustrated in Figure 3.

The electric heating wires are composed of iron/chromium/aluminum alloy. Four heating layers are arranged along the height direction, which are divided into upper and lower units at the midpoint. The upper heating unit and the lower heating unit are connected in parallel, and the structural configuration is shown in Figure 4.



Figure 2. High-temperature solid heat storage and supply system.

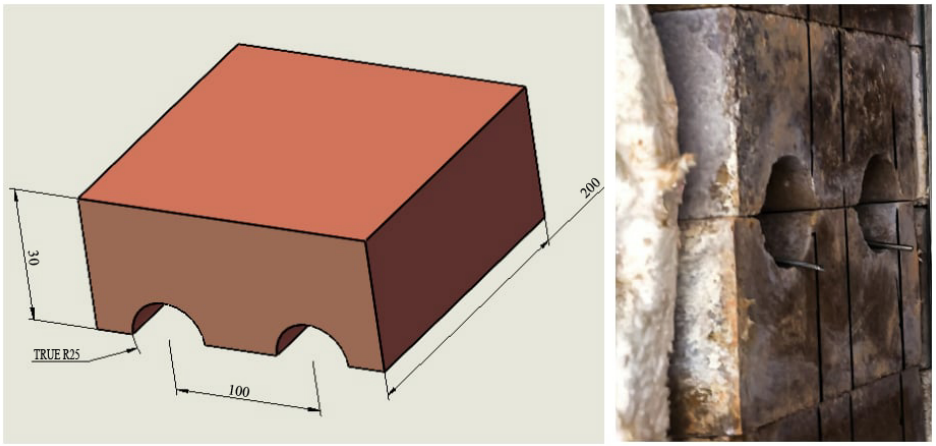


Figure 3. Structural configuration of thermal storage brick.

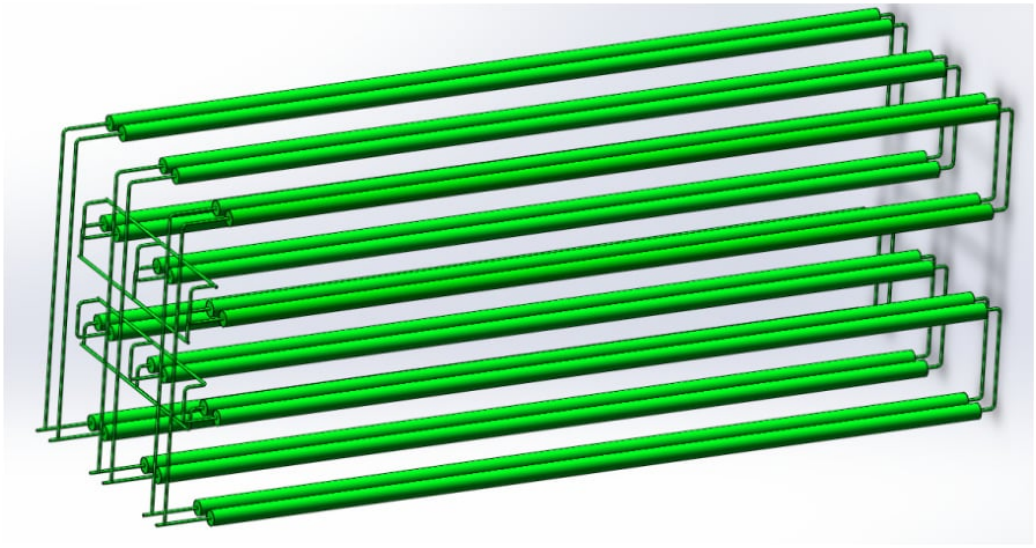


Figure 4. Connection method of electric heating wire.

The distribution of temperature measurement points in different section is shown in Table 1. K-type thermocouples, whose measurement range and accuracy met the requirements of the high-temperature environment above 800 °C, are used in all temperature measurements.

Table 1. Distribution of temperature measuring points.

Measurement Objects	Measurement Points
Saturated-section solid heat storage unit, $T_{u\text{-}sat}$	* Averaged value of five uniformly distributed thermocouples
Superheated-section heat storage unit, $T_{u\text{-}sup}$	* Averaged value of five uniformly distributed thermocouples
Inlet air of saturated-section, T_{aisat}	Thermocouple at inlet of air duct
Outlet air of saturated-section, T_{aosat}	Thermocouple at outlet of air duct
Inlet air of superheated-section, T_{aisup}	Thermocouple at inlet of air duct
Outlet air of superheated-section, T_{aosup}	Thermocouple at outlet of air duct
Saturated steam, T_{ssat}	Thermocouple at outlet of steam pipe
Superheated steam, T_{ssup}	Thermocouple at outlet of steam pipe

* Remarks: The thermocouple is arranged in a "center + up and down, left and right" pattern within the solid thermal storage body, and the arithmetic mean of the readings from 5 measuring points is taken as the representative temperature of the thermal storage unit in that section.

Air and steam flow rates were acquired using high-precision vortex flow transmitters (Rosemount 8800, Emerson, St. Louis, MO, USA). The water flow rate is measured by an electromagnetic flowmeter (Rosemount 8700, Emerson, St. Louis, MO, USA). Steam and system pressures were obtained by averaging the real-time signal of silicon pressure sensors. All the output signals are recorded every 15 s continuously using a data acquisition system (NI DAQ-9174, National Instruments, Austin, TX, USA).

2.2. Experimental Methods

The 3 MWh high-temperature solid heat storage and supply system can be operated in two modes, i.e., direct electric heating steam supply mode and thermal storage mode. In this way, hot water and steam can be supplied on demand under the conditions of valley power and renewable power generation.

(1) Direct electric heating steam supply mode. In this mode, the system acts as a direct steam generator. The thermal storage body is heated and maintained at a constant high temperature by electric resistance wires using external electric power, and steam or

hot water is produced through circulating air. The key aspect of this mode is revealing the effects of circulating air flow rate on the inlet and outlet air temperatures of the heat exchanger, output power, and heat exchange efficiency of each section when the temperature of the thermal storage body is kept constant.

(2) Thermal storage mode. In this mode, the system is used as an energy storage unit. Thermal energy is stored by utilizing valley electricity or surplus power from renewable energy sources, and heat is released on demand when hot water and steam are required. After the thermal storage body is heated to the target temperature, electric heating is terminated, and the system switches to a pure heat-releasing state. Under the condition that the total output power of the system is kept constant, this mode focuses on the dynamic properties of the thermal storage body temperature, inlet and outlet temperatures of circulating air, circulating air flow rate, fan operating frequency and other parameters during the heat releasing process.

A 24 h continuous test of the system was carried out in this paper to simulate the complete "heat storage–heat release" operating cycle. The core performance indicators of the system—including the average electric heat storage power, heat storage capacity, conversion efficiency and heat loss rate—were obtained, and the technical feasibility of the system was verified.

2.3. Measurement and Calculation Methods of Performance Indicators

The primary operating parameters of the system were measured in accordance with the Chinese National Standard, Thermal storage device with electrical input and thermal output (GB/T 39288—2020) [22].

Based on the steady-state and dynamic data collected, the system performance was quantitatively analyzed.

Thermal storage electric power refers to the average electric power input converted into thermal energy and stored in the thermal storage medium per unit time during the operation of a high-temperature solid thermal storage system under electric heating and thermal storage conditions. It is a core parameter reflecting the electric load level of the thermal storage component of the system.

$$P_{al} = \frac{E_4/\tau_4 + E_6/\tau_6}{2} \times 3600 \quad (1)$$

where P_{al} represents the thermal storage electric power, kW; E_4 denotes the power consumption during the first re-energization thermal storage process, kWh; E_6 signifies the power consumption during the second re-energization thermal storage process, kWh; τ_4 represents the energization duration of the first re-energization thermal storage process, s; τ_6 represents the energization duration of the second re-energization thermal storage process, s.

Energy supply power refers to the effective thermal power that can be stably delivered to the user side per unit time when the high-temperature solid thermal storage system is in a state of external heat supply, meeting the needs of heating and steam production. It is the core parameter reflecting the system's heat supply output capacity.

$$P_g = m_{fw} \cdot \left(h_g - h_{fw}\right) \cdot 1000 \Big/ 3600 \quad (2)$$

where m_{fw} represents the feedwater mass flow rate, t/h; h_{fw} represents the enthalpy value of feedwater, kJ/kg;

Thermal storage capacity refers to the maximum effective heat that can be stably outputted externally during a complete heat release cycle after the high-temperature solid thermal storage system is heated up to its rated maximum thermal storage temperature

(i.e., the maximum effective heat release of the system). It is a core parameter characterizing the thermal storage scale of the system.

$$Q_{mdlv} = \frac{m_{fw}(h_{st} - h_{fw})\tau_5}{3600} \quad (3)$$

where Q_{mdlv} represents the thermal storage capacity, MWh; h_{st} represents the enthalpy value of superheated steam, kJ/kg; τ_5 represents the duration of the second heat release process, s.

System electric-to-thermal conversion efficiency refers to the ratio of the total effective heat output to the total electric energy consumed throughout the entire cycle after a high-temperature solid thermal storage system completes a complete heat storage/discharge cycle. It is a core performance indicator for measuring the energy utilization level of the system.

$$\eta = \frac{Q_{mdlv} \cdot 1000}{(E_4 + E_6)/2 + E_5} \times 100\% \quad (4)$$

where η represents the electric-to-thermal conversion efficiency, %; E_5 represents the power consumption during the second discharge process, kWh.

Uncertainty analysis is conducted on the main measuring instruments. The uncertainty of the K-type thermocouple, vortex flowmeter, electromagnetic flowmeter and pressure sensor is within 2.5%, 1.0%, 0.5% and 1.8% respectively in this paper. Through uncertainty propagation calculations, the expanded uncertainties ($k = 2$) for thermal power, thermal storage capacity, and thermal efficiency were ±3.8%, ±2.9%, and 1.5%, respectively.

3. Results and Discussion

3.1. Direct Electric Heating Steam Supply

In direct electric heating steam supply mode, the thermal storage tank is maintained at a high temperature. When the thermal storage tank is maintained at a high temperature, efficient heat output can be achieved with a low air flow rate. However, variations in air flow significantly affect the fluid heat transfer characteristics and system heat transfer rate. Therefore, it is necessary to investigate the influence of the air flow rate on the heat transfer process.

The heat release process of the system is dominated by convective heat transfer between the high-temperature heat storage body and circulating air. According to the principle of convective heat transfer, the heat transfer rate is affected by temperature difference, air velocity, heat transfer area and so on. Figure 5 presents the curves showing the influence of circulating air flow rate on the inlet and outlet air temperatures as well as output power of each heat exchange section when the heat storage body in the saturated section is maintained at 900 °C. It can be observed from the figure that as the circulating air flow rate increases from 1520 Nm^3/h to 7800 Nm^3/h, the outlet air temperature of the heat storage body gradually decreases from 600 °C to 300 °C. With the rising circulating air flow rate, the temperature difference between the inlet and outlet air of the heat storage body rapidly drops from 350 °C to 70 °C. This is because the increased air velocity shortens the residence time of per unit volume of air inside the heat storage body, reducing the heat absorption and thereby lowering the inlet/outlet temperature difference.

Figure 6 shows the curves indicating the influence of circulating air flow rate on the inlet and outlet air temperatures and output power of each heat exchange section when the heat storage body in the superheated section is kept at 900 °C. As the circulating air flow rate increases from 2800 Nm^3/h to 8000 Nm^3/h, the outlet air temperature of the heat storage body gradually decreases from 600 °C to 500 °C, and the inlet/outlet air temperature difference of the heat storage body decreases gradually from 35 °C to 10 °C. The mechanism

of the reduction in inlet/outlet temperature difference is basically consistent with that of the saturated section.

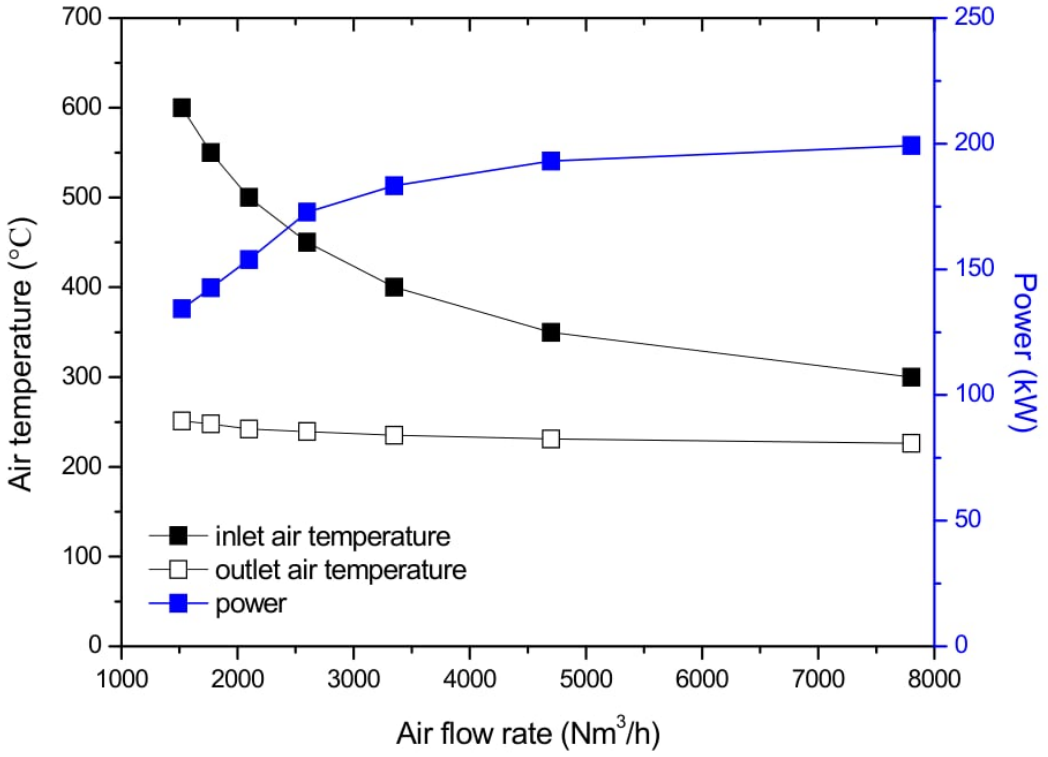


Figure 5. Relationship curves of circulating air temperature and output power versus circulating air volume in the saturation segment.

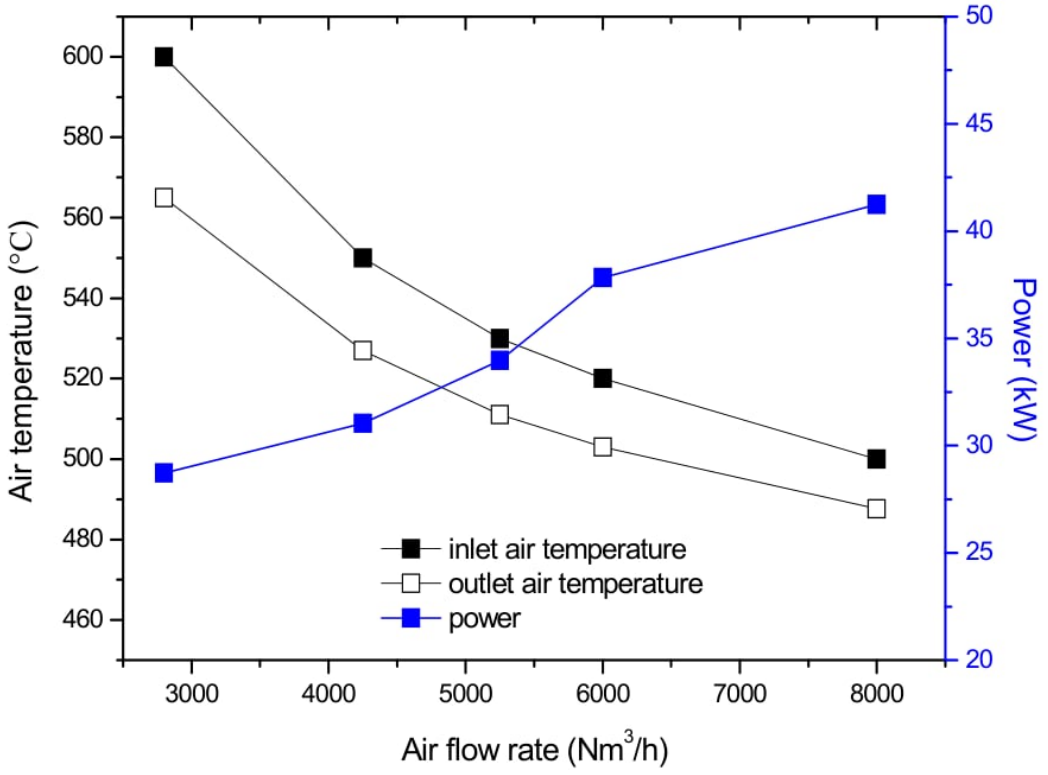


Figure 6. Variation curves of circulating air temperature and output power in the superheating section with circulating air volume.

It is worth noting that the heat transfer intensity of circulating air in the superheated section is obviously lower than that in the saturated section. This arises from two factors: on one hand, the heat transfer area of the superheated section is smaller than that of the saturated section; on the other hand, the temperature difference between the inlet air and the heat storage body in the superheated section is relatively small. Therefore, the inlet/outlet temperature difference of circulating air in the superheated section is markedly lower than that in the saturated section under high air velocity.

It can be found from Figures 5 and 6 that the output power of the saturated section rises from 134 kW to 199 kW, and the output power of the superheated section increases from 29 kW to 41 kW. Although the rise in circulating air flow rate reduces the inlet/outlet temperature difference of circulating air, the enhanced turbulence improves the heat transfer rate. The mechanism of how heat transfer rate varies with air flow rate lies in the fact that the increase of flow rate raises the Reynolds number, which enhances the convective heat transfer and consequently leads to a rise in heat transfer rate. Meanwhile, the residence time of air inside the regenerator is shortened, resulting in a smaller temperature rise of air, but this will cause an increase in fan power consumption.

3.2. Energy Storage Supply Mode

In this section, the system acts as an energy storage device during the off-peak electricity heat storage and steam supply process. A constant total output power is set in the experiments to investigate how adaptive variable-frequency fan regulation maintains the target output while heat is continuously released from the heat storage body and its temperature decreases naturally. The variation in state parameters is recorded throughout the tests. By examining the temperature decay curve of the heat storage body, fan parameters and steam parameters, this section verifies that stable steam supply can be maintained by the proposed system as the state of the heat storage body evolves. The heat charging stage refers to the process in which the heat storage body is electrically heated, and its theory is relatively straightforward. This study focuses on the variation relationship among the output heat, heat storage body temperature and circulating air under the heat storage mode.

It can be seen from Figure 7 that with the continuous heat output, the temperature of the saturated-section solid heat body gradually decreases from 800 °C to 745 °C within 1.5 h, and the inlet/outlet temperature difference of the circulating air decreases gradually from 360 °C to 267 °C. At the initial stage of heat output, a large temperature difference is observed between the heat storage body in the saturated section and air, which provides a strong heat transfer driving force. This results in the high outlet temperature of circulating air and a large inlet/outlet temperature difference. As the temperature of the saturated-section solid heat body gradually drops, the heat transfer temperature difference between the heat storage body and circulating air is reduced, which lowers the heat absorption per unit volume of circulating air. Therefore, to compensate for the weakened heat transfer of circulating air caused by the temperature drop of the heat storage body, it is necessary to increase the circulating air flow rate to maintain stable output thermal power. As illustrated in Figure 7, the circulating air flow rate is increased from 1530 m^3/h to 2062 m^3/h to keep the output heat constant.

Figure 8 shows the time-dependent variations in heat storage body temperature, inlet and outlet air temperatures, and air flow rate in the superheated section with an initial heat storage body temperature of 790 °C, when stable output power is maintained. It can be observed from Figure 8 that with continuous heat output, the temperature of the heat storage body gradually decreases from 790 °C to 722 °C within 1.5 h, and the inlet/outlet temperature difference of circulating air gradually drops from 156 °C to 99 °C. To maintain constant heat output, the circulating air flow rate is increased from 880 m^3/h to 1384 m^3/h.

Its heat transfer principle and regulation mechanism are similar to those of the saturated section, which will not be repeated here.

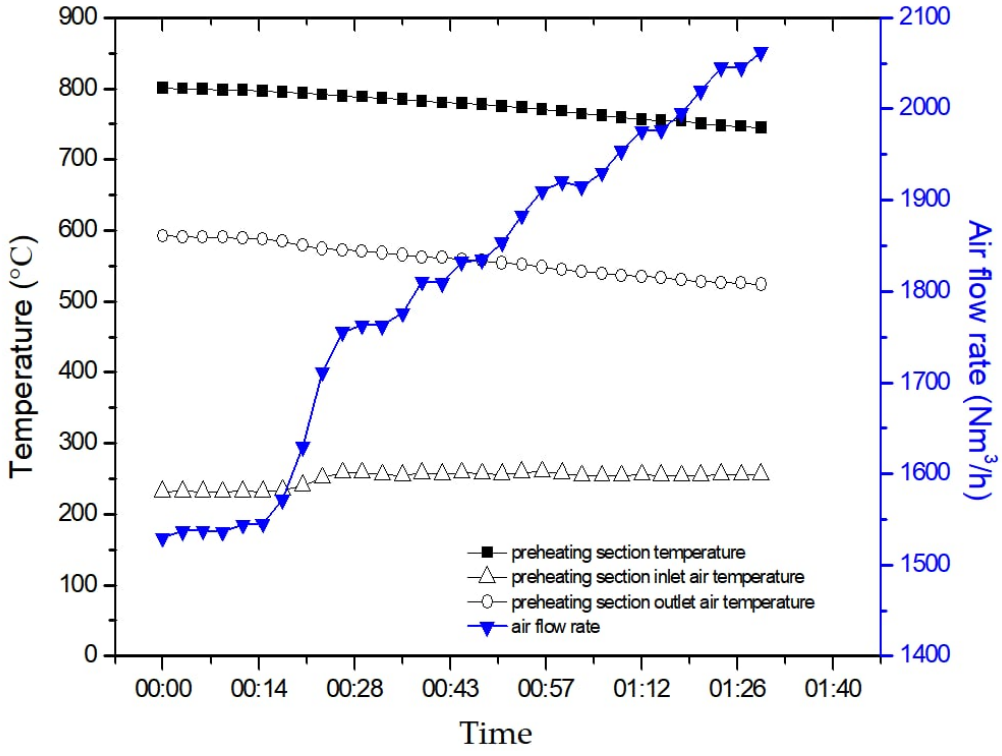


Figure 7. Saturation section temperature and air volume.

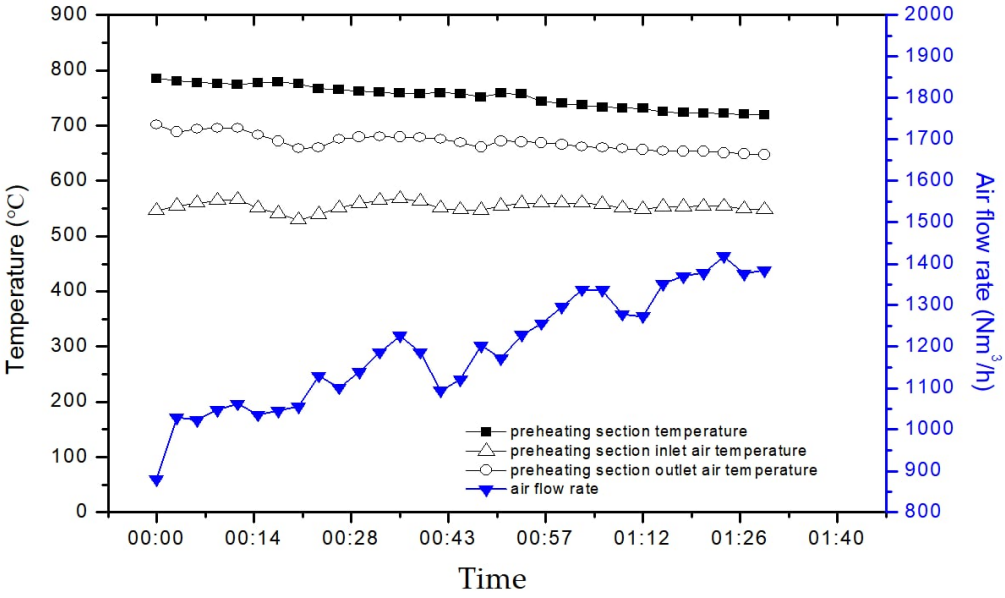


Figure 8. Superheating section temperature and air volume.

Figure 9 presents the variation in temperature and pressure of the generated superheated steam during the above 1.5 h heat release process. It can be seen from the figure that the superheated steam temperature is maintained at approximately 450 °C with a maximum temperature difference of only 18.8 °C. The pressure of superheated steam stays at around 2 MPa, and the maximum pressure deviation is merely 81 kPa. This indicates that the system can keep the parameters of the output superheated steam constant by real-time control of the circulating air flow rate.

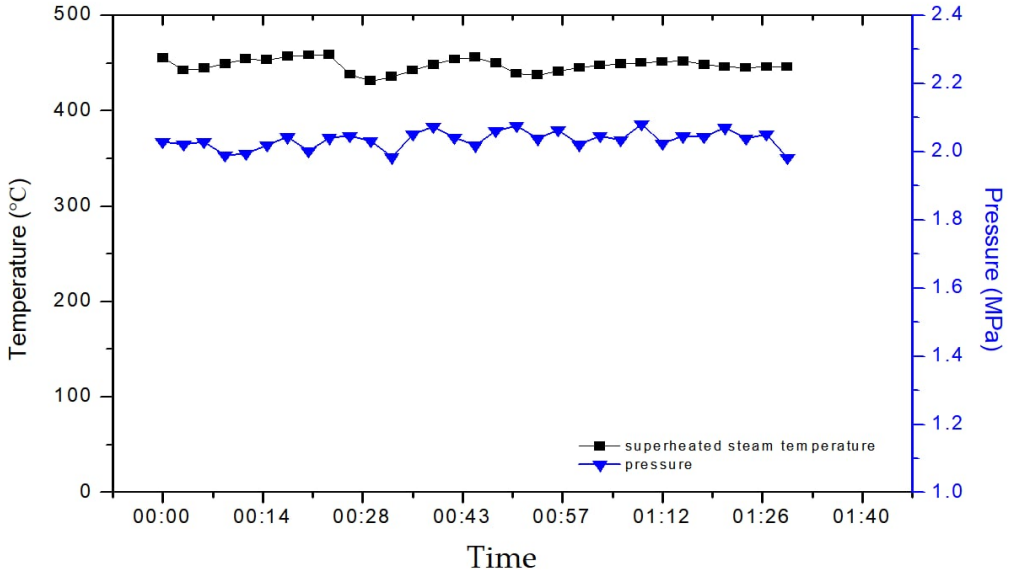


Figure 9. Superheated steam parameter curve.

Figure 10 shows the superheated steam production rate and output power during the above 1.5 h heat release process. It can be observed from the figure that the superheated steam production rate is maintained at approximately 0.23 t/h, with a variation range of only −7.46%. Meanwhile, the output power of superheated steam remains at roughly 207 kW, with a variation range of merely −7.43%. It can therefore be concluded that the system maintains a stable superheated steam production rate with the steady-state deviation within ±8%.

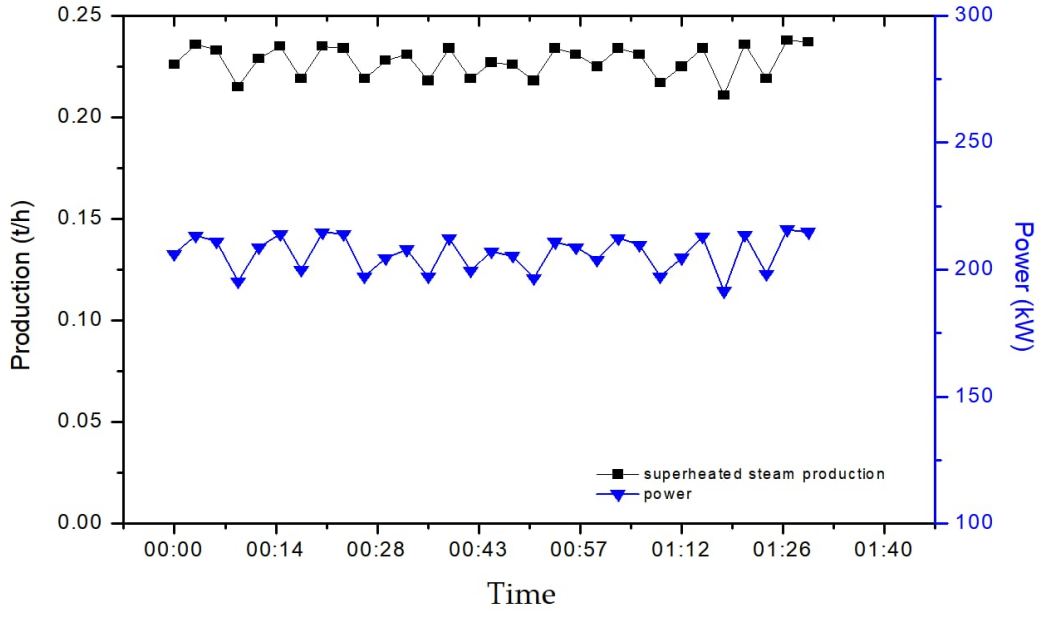


Figure 10. Superheated steam production and output power curve.

3.3. System Performance

A 24 h continuous operation test of the high-temperature solid heat storage and supply system was carried out to complete a full practical working cycle as shown in Figure 11, and the overall system performance was investigated. A test with two charge/discharge cycles was completed within 24 h. Heat charging was initiated at 22:00 during the off-peak electricity period. The heat storage bodies of the saturated section and superheated section

were heated starting from 440 °C and 490 °C, respectively. Both sections reached 850 °C after 4 h of heat charging and were kept at constant temperature until 07:00 on the next day. When heat demand was required, the system released heat slowly in the form of superheated steam until 11:00. At the end of heat discharge, the temperature of the superheated section decreased to 650 °C and that of the saturated section dropped to 600 °C. Heat charging was restarted at the next off-peak period (11:00) following an identical procedure, and the heat storage bodies were heated to 850 °C within 5 h and maintained at this temperature until 19:00. To meet the nighttime heat demand, rapid heat discharge was performed until 22:00, and the temperature of the heat storage bodies decreased to about 500 °C.

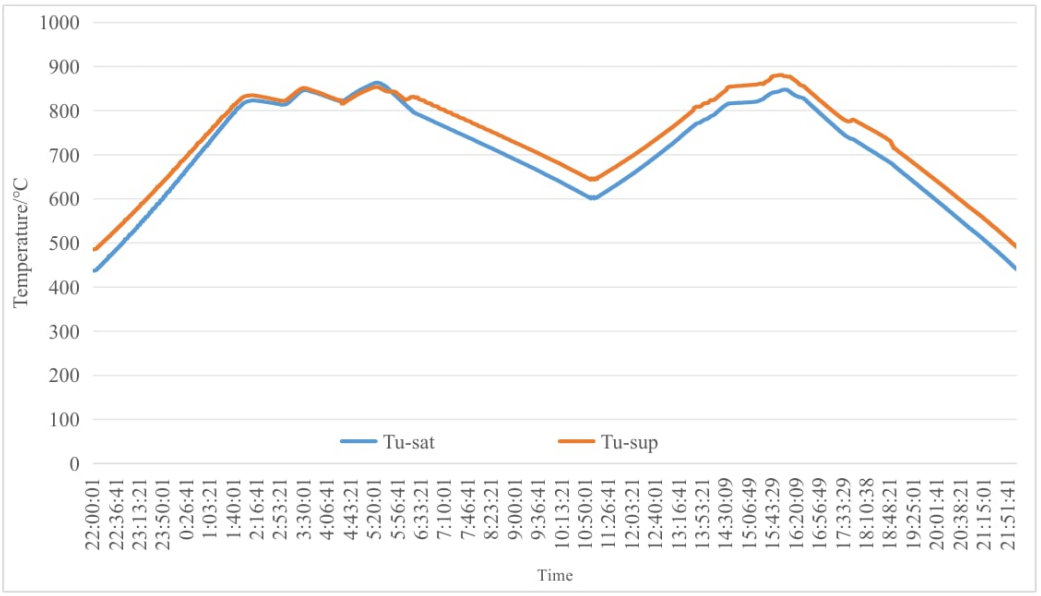


Figure 11. Temperature variation curve of the regenerator.

The main performance parameters of the system are listed in Table 2. Under the maximum heating power, full heat charging can be achieved within 5 h. The system has a heat storage capacity of approximately 3.14 MWh and can generate superheated steam at 2 MPa and 450 °C, while being capable of supplying saturated steam and hot water simultaneously.

The containerized 3 MWh high-temperature solid heat storage and supply system features the advantages of mobility and rapid deployment. The system was transported from Binzhou, Shandong Province, to Hengyang, Hunan Province, over a distance of approximately 1500 km. Figure 12 shows the transportation arriving at the site. On-site operation demonstrates that the system can be rapidly commissioned at the destination to supply hot water and steam on-site.

This system achieves compact integration while maintaining high thermal performance. However, this solution still has several limitations: compared to large-scale thermal storage devices applied in industrial parks or power stations, it has a relatively higher proportion of heat loss due to its larger specific surface area; the process of this system complies with Chinese National Standard, Thermal storage device with electrical input and thermal output (GB/T 39288—2020), and the power consumption of MgO bricks, heating elements, and fan systems is comparable to that of existing energy storage systems.

Table 2. System performance index requirements of the 3 MWh solid heat storage system.

Item	Unit	Value
Maximum heat storage temperature	°C	910
Superheated steam temperature	°C	450
Superheated steam pressure	MPa	2
Maximum heat storage electric power	kW	700
Output hot water power	kW	628
Output superheated steam thermal power	kW	303
Heat storage capacity (maximum effective heat release)	MWh	3.14
System electro-thermal conversion efficiency	%	97.84
Power consumption during the first heating process after re-energization E_4	MWh	3.26
Power consumption of the exothermic process E_5	MWh	0.03
Power consumption of the second heating process during the second power-on E_6	MWh	3.10
Heating water supply quality and flow rate	t/h	15.89
Heating hot water temperature	°C	79



Figure 12. Portable device.

4. Conclusions

(1) In the experimental research on the direct electric heating steam supply mode, the system continuously maintains the thermal storage body at a preset high temperature through electric heating, and produces steam or hot water directly relying on the convective heat transfer process between circulating air and the thermal storage body as well as heat exchange components. The experiment quantitatively reveals the influence law of circulating air flow rate on heat transfer processes and system output characteristics under constant-temperature thermal storage conditions: The core mechanism of the system's heat release process in this mode is convective heat transfer between the high-temperature thermal storage body and circulating air. Variations in circulating air flow rate directly affect the heat absorption capacity of air per single circulation cycle and the overall heat transfer performance by changing the residence time of unit volume of air in the air flow channels formed by stacked thermal storage bricks. When the thermal storage body in the saturated section is maintained at a constant temperature of 900 °C, as the circulating air flow rate increases from 1520 to 7800 Nm^3/h, the outlet air temperature of the saturated-section thermal storage body gradually drops from 600 °C to 300 °C, and the air temperature difference between the inlet and outlet of the thermal storage body narrows rapidly from 350 °C to 70 °C. The heat exchange efficiency and output power of each heat exchange link in both saturated and superheated sections present a significant quantitative correlation with the

circulating air flow rate, and this law can provide direct experimental support for operating parameter matching and rapid output power regulation in direct heat supply scenarios.

(2) In the experimental study on the thermal storage heating mode, the system first heats the thermal storage body to the preset target temperature using valley electricity or surplus power from renewable energy sources, then cuts off electric heating to enter the pure heat-releasing state, and supplies hot water and steam to external users on demand. The experiment identifies the dynamic characteristics of the full-cycle heat release process under the stable-power supply target, and verifies the stable energy supply performance of the adaptive air volume regulation mechanism: During the pure heat release process, the temperature of the thermal storage body decreases gradually with continuous heat output; if the system operates with a fixed air flow rate, the output power will decline continuously due to the progressive shrinkage of the heat transfer temperature difference. Specifically, during the 1.5 h continuous heat discharge process, the temperature of the saturated-section heat storage body gradually decreased from 800 °C to 745 °C, with the circulating air flow rate correspondingly increased from 1530 to 2062 m^3/h; in the superheated section, the heat storage body temperature decreased from 790 °C to 722 °C, with the circulating air flow rate increased from 880 to 1384 m^3/h. The system is capable of stably outputting superheated steam above 450 °C.

(3) Experiments with two charge/discharge cycles within 24 h indicate that the system can adapt to the peak/valley electricity cycle in China and stably generate superheated steam at 450 °C. The electro-thermal conversion efficiency reaches 97.84%. After long-distance transportation over 1500 km, the system can be rapidly commissioned at the destination, which demonstrates the advantage of its mobility.

Author Contributions: Conceptualization, D.G., H.Y. and R.L.; methodology, D.G., H.Y. and R.L.; validation, D.G., H.Y. and L.W.; formal analysis, D.G., L.W. and Z.W.; investigation, D.G., L.W. and Z.W.; resources, H.Y. and L.Y.; data curation, D.G., H.Y. and L.Y.; writing—original draft, D.G.; writing—review and editing, H.Y. and R.L.; visualization, R.L.; supervision, H.Y. and L.Y.; project administration, L.Y.; funding acquisition, L.Y. All authors have read and agreed to the published version of the manuscript.

Funding: This work was supported by China Yangtze Power Co., Ltd. (No. Z342402007).

Data Availability Statement: The original contributions presented in the study are included in the article, and further inquiries can be directed to the corresponding author.

Conflicts of Interest: Authors Hongmei Yin, Lin Wang, Ziwei Wang, and Liming Yang were employed by the Science and Technology Research Institute, China Three Gorges Corporation. Authors Dajiang Guo and Rujie Liu were employed by Three Gorges Electric Energy Co., Ltd. The remaining authors declare that the research was conducted in the absence of any commercial or financial relationships that could be construed as potential conflicts of interest.

References

1. Seyitini, L.; Belgasim, B.; Enweremadu, C.C. Solid state sensible heat storage technology for industrial applications—A review. *J. Energy Storage* **2023**, *62*, 106919. [CrossRef]
2. Zeng, G.; Ji, Y.; Fu, J. Research Status, Hot Trends and Application Progress of Thermal Energy Storage Technology. *Proc. CSEE* **2023**, *43*, 127–142.
3. Ma, M.; Zhang, K.; Chen, M. Research status and prospects of solid electric heat storage technology. *Zhejiang Electr. Power* **2023**, *42*, 25–33.
4. Ghassemi Kakroudi, M.; Pourmohammadie Vafa, N.; Shahedi Asl, M.; Shokouhimehr, M. Effects of SiC content on thermal shock behavior and elastic modulus of cordierite—Mullite composites. *Ceram. Int.* **2020**, *46*, 23780–23784. [CrossRef]
5. Xu, J. Study on Heat Transfer Enhancement of Basalt Fiber Bundle Heat Storage in Mixed Channel. Master's Thesis, Southeast University, Nanjing, China, 2021.

6. Schwarzmayr, P.; Birkelbach, F.; Walter, H.; Hofmann, R. Standby efficiency and thermocline degradation of a packed bed thermal energy storage: An experimental study. *Appl. Energy* **2023**, *337*, 120917. [CrossRef]
7. Zan, X.; Yin, S.; Wang, T.; Liu, C.; Tong, L.; Wang, L.; Wu, C.Y. Analysis of heat storage and release characteristics in high-temperature solid heat storage devices with multiple face channels. *Appl. Therm. Eng.* **2025**, *274*, 126576. [CrossRef]
8. Liu, X.; Xu, L.; Liu, J.; Chou, P.; Wang, G. Study and optimization of charging characteristics of high-temperature solid heat storage device. *Acta Energiae Solaris Sin.* **2025**, *46*, 342–350. [CrossRef]
9. Lai, Z.; Hou, C.; Chen, J.; Guo, X.; Han, G.; Zhang, K.; Ding, L.; Lv, H. Experimental study on energy storage characteristics of packed bed using different solid materials. *J. Energy Storage* **2024**, *100*, 113701. [CrossRef]
10. Hou, Z. Research on Optimization Design of Convection Tube Bundle in Solid Thermal Storage Electric Boiler. Master's Thesis, Hebei University of Architecture, Shijiazhuang, China, 2024.
11. Sun, Y.; Niu, J.; Xu, H.; Liu, Y.; Yang, Y.; Xu, F. A study on optimization of the air supply system for the electric heating solid heat storage unit. *J. Comput. Methods Sci. Eng.* **2022**, *22*, 2319–2342. [CrossRef]
12. Li, T.; Zou, T.; Li, H. Research on technical Optimization of solid regenerative electric Boiler. *J. Phys. Conf. Ser.* **2022**, *2247*, 012015. [CrossRef]
13. Tian, Y.; Yu, M.; Mao, Y.; Cui, P.; Zhang, W.; Zhuang, Z. Study on long-term operation characteristics of the medium-deep ground source heat pump system with solar heat storage. *Appl. Therm. Eng.* **2024**, *241*, 122345. [CrossRef]
14. Wang, S.; Deng, X.; Wang, J.; Li, M. Heat transfer analysis of deep coaxial geothermal heat exchangers: Insights into heat-flux distribution on borehole wall. *Energy Built Environ.* **2025**, *6*, 596–606. [CrossRef]
15. Huang, Y.; Cao, D.; Sun, D.; Liu, X. Experimental and numerical studies on the heat transfer improvement of a latent heat storage unit using gradient tree-shaped fins. *Int. J. Heat Mass Transf.* **2022**, *182*, 121920. [CrossRef]
16. Ren, F.; Du, J.; Cai, Y.; Guo, J.; Liu, Y.; Zhang, D.; Li, M. Study on thermal performance of a new optimized snowflake longitudinal fin in vertical latent heat storage. *J. Energy Storage* **2022**, *50*, 104165. [CrossRef]
17. Cheng, M.; Cheng, T.; Fu, Q. Optimal dispatching method for regenerative electric heating system considering the heating reliability and power constraint of distribution network. *Electr. Meas. Instrum.* **2024**, *61*, 115–121.
18. Ji, M.; Lv, L.; Huang, S.; Zhang, A.; Zhou, H. Experimental study of thermal energy storage system for solid particles/heat transfer oil in shell and tube heat exchangers with H-shaped fins. *J. Clean. Prod.* **2024**, *434*, 139943. [CrossRef]
19. Liu, X. Optimization Analysis of Heat Charging Process of Heat Storage Unit of High-Temperature Solid Heat Storage Device for Energy Storage Power Station. Master's Thesis, Xinjiang Agricultural University, Urumqi, China, 2025.
20. Liu, F.; Zhao, B.; Wang, Y.; Wu, W.; Zhang, G. Molten Salt Thermal Storage-Based Superheated Steam Power Generation Technology and Its Economic Analysis. *Power Stn. Aux. Equip.* **2025**, *46*, 5–9.
21. Ye, Z.; Han, K.; Wang, Y.; Li, C.; Zhao, C.; He, J.; Zhang, L. Techno-economic assessment and mechanism discussion of a cogeneration shared energy storage system utilizing solid-state thermal storage: A case study in China. *J. Energy Storage* **2024**, *84*, 110843. [CrossRef]
22. *GB/T 39288—2020*; Thermal storage device with electrical input and thermal output. National Standardization Administration of China: Beijing, China, 2020.

Disclaimer/Publisher's Note: The statements, opinions and data contained in all publications are solely those of the individual author(s) and contributor(s) and not of MDPI and/or the editor(s). MDPI and/or the editor(s) disclaim responsibility for any injury to people or property resulting from any ideas, methods, instructions or products referred to in the content.